PHOTOELECTRON SPECTROSCOPY ON SMALL ANIONIC COPPER-CARBONYL CLUSTERS

Jörg STANZEL[1], Emad F. AZIZ[2], Matthias NEEB[3,*], Wolfgang EBERHARDT[4]

BESSY, Albert-Einstein Str. 15, D-12489 Berlin, Germany; e-mail: [1] stanzel@bessy.de, [2] emad@bessy.de, [3] neeb@bessy.de, [4] eberhardt@bessy.de

Received October 4, 2006
Received November 21, 2006

Dedicated to Professor Jaroslav Koutecký.

Anion photoelectron spectroscopy in combination with density functional theory (DFT) calculations has been used to study mono- and dinuclear copper-carbonyl clusters $Cu_n(CO)_m^-$ (n = 1, 2; m = 2–5). The adiabatic detachment energies of the anions have been measured which correspond to the electron affinities of the respective neutral species. The corresponding values are 0.95 eV for $Cu(CO)_2$, 1.02 eV for $Cu(CO)_3$, 1.04 eV for $Cu(CO)_4$, 1.43 eV for $Cu_2(CO)_4$, and 1.19 eV for $Cu_2(CO)_5$. All spectra exhibit a pronounced vibrational fine structure on the adiabatic photodetachment peak. The energy splitting is close to the energy of the C–O stretching vibration of the neutral cluster (final state). The DFT calculations clearly indicate that in all clusters the highest occupied molecular orbital (HOMO) is a CO-derived π* orbital. Furthermore the calculations are used to give insight into geometry, frontier orbitals, vibrational frequencies and spin multiplicity of the neutral and anionic clusters.
Keywords: Copper; Carbonyl complexes; Clusters; Photoelectron spectroscopy; Ab inition calculations; DFT.

The combination of cluster anion photoelectron spectroscopy with quantum chemical ab initio calculations is an example of fruitful collaboration between theorists and experimentalists. Photoelectron detachment spectra of mass-selected cluster anions contain valuable information on the electronic valence structure of clusters. Experimentally obtained parameters like the adiabatic detachment energy, the HOMO-LUMO-bandgap, and vibrational frequencies are eagerly used by theorists to verify the reliability of their cluster calculation. As experimental methods are rare to directly reveal the structure of free clusters, quantum chemical calculations are in most cases the only way to obtain information on the cluster geometry and its relation to the electronic structure. Prof. Koutecký is one of the pioneers in

doi:10.1135/cccc20070001

modeling the electronic structure and geometry of small metal clusters including multiple citations on sodium[1–4] and silver cluster anions[5].

Transition-metal carbonyls are main constituents of modern organometallic chemistry and their study gives basic insight into the bonding of metals with adsorbate molecules. The interaction between a metal and adsorbate molecules is of fundamental interest in surface and cluster science as well as for nanocatalytic reaction on small clusters. For instance, Cu-based catalysts are used at much lower costs for methanol production by CO hydrogenation[6]. Copper clusters are believed to play an essential part in the catalytic cycle. Generally, it is widely accepted that the carbonyl bond (M–CO) in transition-metal carbonyls is mainly formed by ligand-to-metal σ-donation and metal-to-ligand π-back-donation[7]. The donation-to-back-donation ratio is a matter of concern and it turns out that the donation is principally less important for the M–CO bond strength than back-donation. This arises mainly by the fact that a strong orbital repulsion exists between the metal 4s and CO 5σ orbitals[8]. The σ contribution is the smaller the less unfilled d orbitals are available in the metal. Thus the Cu–CO metal-ligand bond is of principal interest because the Cu atom has a closed d-shell. Any charge redistribution from the 4s valence orbital into the 3d-orbital space is therefore impossible for Cu in order to minimize the large repulsive interaction between the 4s and 5σ orbitals. Such intrametal s–d charge redistribution is the principal reason for the formation of thermally stable carbonyl clusters made from open d-shell transition metals like Fe, Ni, Cr and V but not from Cu [8,9]. However, in a cluster beam at sufficiently low temperatures (T_{vib} ~ 200 K)[10], we were able to produce a series of Cu-carbonyls. Here we report on the electron structure of the smallest Cu-carbonyl aggregates namely mono- and dimetallic copper-carbonyl clusters.

EXPERIMENTAL

The experimental setup is described in detail elsewhere[11]. Copper-carbonyl complexes are produced in a pulsed laser vaporization source. The second harmonic of a Nd:YAG laser is focused on a rotating copper rod producing a plasma. The plasma is cooled during supersonic expansion within He carrier gas. The He is inserted using a solenoid valve (backing pressure 20 bar). CO adsorption is achieved by a second pulsed valve downstream of the expanding cluster beam operating with a backing pressure of ~1 bar of purified CO gas. Cluster anions are mass-selected using a Wiley–McLaren time-of-flight spectrometer. The mass-selected bunches of cluster anions are decelerated before entering the interaction region of a magnetic bottle time of flight spectrometer. The energy resolution of the spectrometer ranges from around 10 meV for the electron kinetic energy E_{el} = 0.5 eV to 40 meV for E_{el} = 3 eV. For photodetachment we use the second harmonic of a pulsed Ti:Sa laser (800 nm, 3.1 eV, energy per pulse 100 μJ). The spectrometer has been calibrated using the peak posi-

tions of the copper and tungsten monomer. The binding energies of the corresponding atoms were taken from Moore[12].

COMPUTATIONAL

The program package Gaussian03 [13] has been used for the calculations. Density functional theory has been applied in combination with an augmented double ζ basis set and B3LYP functional. This functional and basis set were shown to give good results for the calculations on small Cu-carbonyls[14,15]. Geometry optimization were performed on different geometries with high and low symmetry followed by frequency calculations. The molecular orbitals (HOMO-1, HOMO, LUMO) are visualized by Gaussian View package, where 0.02 isosurface was used for all molecular orbitals.

RESULTS AND DISCUSSIONS

Photodetachment spectra of the monocopper-carbonyl clusters are shown in Fig. 1b–1d. The photoelectron spectrum of the negatively charged copper atom is well known from literature (e.g. Ganteför et al.[16]) and is shown for comparison in Fig. 1a. The first photodetachment line of Cu^- (peak at 1.23 eV) corresponds to the transition from the ground state of the Cu anion into the ground state of the neutral atom, e.g. $3d^{10}4s^2 \rightarrow 3d^{10}4s^1$, and corresponds to the electron affinity of the copper atom. The single line is due to transition into the doublet final state of the neutral atom which is characterized by a singly occupied valence s-shell $4s^1$. The second photodetachment line seen at 2.6 eV corresponds to the transition from the anionic ground state into the first excited state of Cu_1, e.g. $3d^{10}4s^2 \rightarrow 3d^94s^2$. The energy difference of 1.4 eV with respect to the adiabatic photodetachment peak is equal to the HOMO-LUMO gap of the neutral Cu atom, e.g. $3d^{10}4s^1 \rightarrow 3d^94s^2$. The energy difference fits perfectly with the value of 1.39 eV for the $^2D_{5/2}$ final state as given by Moore[12]. The third peak seen in Fig. 1a is also due to emission from the 3d orbital, e.g. $3d^{10}4s^2 \rightarrow 3d^94s^2$ (^2D). The blue shift of 0.2 eV with respect to the peak at 2.6 eV arises from spin-orbit coupling of the 3d hole and agrees well with the *J*-splitting between $^2D_{5/2}$ and $^2D_{3/2}$ of 0.25 eV as given by ref.[12].

Upon CO adsorption, as displayed in Fig. 1b, the first peak shows a well resolved vibrational progression (v = 0–2) which arises from Franck–Condon excitations of neutral $Cu(CO)_2$. The vibrational energy is 241 ± 10 meV (1936 ± 81 cm^{-1}) and corresponds to the energy of the C–O stretching vibration. With respect to free CO (269 meV)[17], the vibrational energy of the adsorbed CO ligand in $Cu(CO)_2$ is lowered by ~28 meV. This indicates a destabilization of the C–O bond. The adiabatic detachment energy (e.g. electron binding energy at v = 0) amounts to 0.95(4) eV and is somewhat

lower than the corresponding value of the Cu atom. The next lower state at 2.85 eV represents the first excited state of neutral $Cu(CO)_2$. Thus the HOMO-LUMO gap is 2 eV and more than 0.5 eV larger than that of the Cu atom. This is an indication of the s–d repulsion mentioned in the introduction.

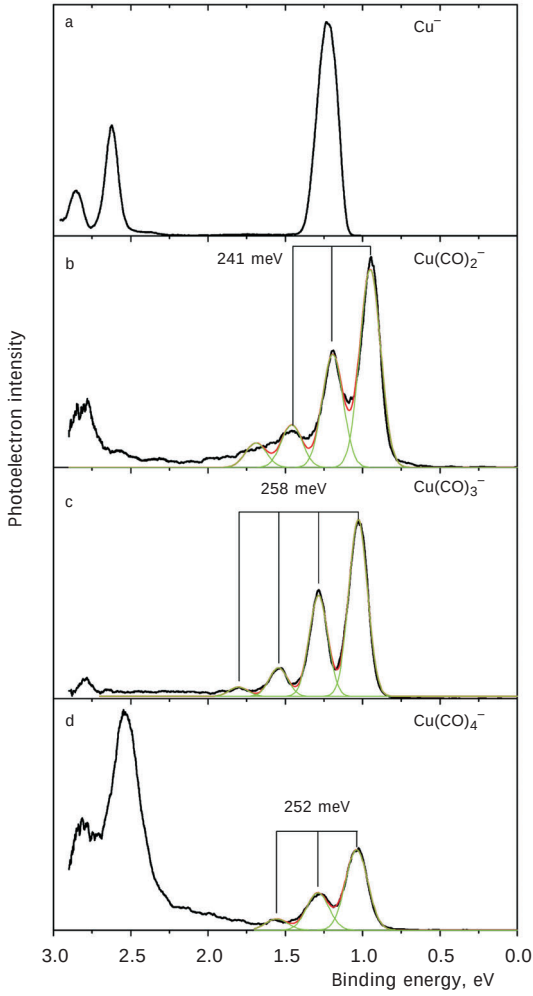

FIG. 1

Photoelectron spectra of Cu_1^- (a), and the monocopper-carbonyl clusters $Cu(CO)_2^-$ (b), $Cu(CO)_3^-$ (c) and $Cu(CO)_4^-$ (d) at a photon energy of 3.12 eV. The vibrational energy splitting is indicated by vertical black lines and the vibrational fine structure is fitted by a sum (red line) of individual Gaussian functions (green line). The experimental spectrum is shown in black

Figure 2 shows the calculated frontier orbitals of neutral and anionic $Cu(CO)_2$ in $D_{\infty h}$ symmetry (calculated ground state structure for both species). These oritals have all π symmetry and are composed of the degenerate $2\pi^*$ orbitals of CO. Note that the HOMO does not overlap with any Cu orbital. This agrees well with the observed vibrational progression on the first photodetachment peak which is not disturbed by any low-frequency mode derived from the Cu–C bond. As can be seen by the density plots of the HOMO (Fig. 2a, 2d), the two C atoms on either side of the central Cu atom hybridize with each other without interfering with the orbitals of the central Cu atom. The HOMO thus leads to a constructive overlap between the two separated CO ligands via a banana-like C–C bond. On the other hand, the HOMO is of antibonding character with respect to the C–O bond. This makes the reduction of the observed C–O vibrational energy plausible as the antibonding character weakens the C–O bonding. Note that the antibonding π* orbital is vacant in free CO while it is occupied if CO is attached to Cu. The filling of the CO-derived π* orbital arises from charge backdonation from the Cu atom towards the CO ligands[7,14]. The measured vi-

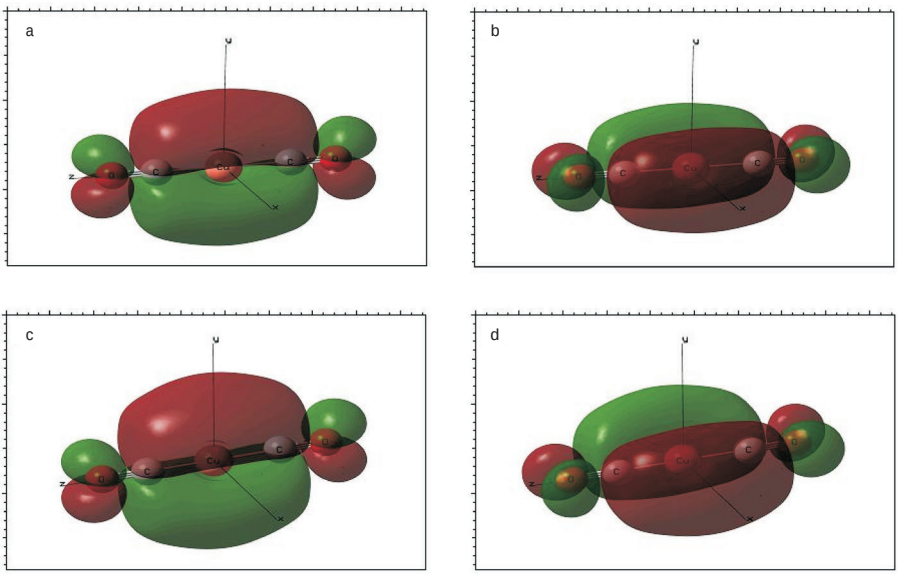

FIG. 2
Orbital contour plot of $Cu(CO)_2$ (upper panel) and $Cu(CO)_2^-$ (lower panel). HOMO (a), LUMO (b), HOMO-1 (c), HOMO (d). The neutral cluster has a doublet electron configuration while the anion has a triplet ground state

brational energy (241 ± 10 meV) fits very well the calculated C–O stretching vibration in $Cu(CO)_2$ (out of phase with respect to the two CO ligands) which is 240 meV. Within the error bars, however, the measured frequency could even correspond as well to the calculated totally symmetric C–O stretching mode (250 meV). This Raman mode would indeed be much more likely considering the high symmetry of the involved orbitals. The experimentally observed Franck–Condon progression indicates that the equilibrium distance of the neutral form and anion is changed. As $\nu = 0$ is the maximum of the Franck–Condon progression, the internuclear shift is expected to be rather small. Note that the anionic cluster has been calculated in its triplet ground state which is by ~0.5 eV more stable than the singlet ground state. The triplet configuration is also the reason why the anionic cluster prefers the linear symmetry. Upon photodetachment, the singly occupied HOMO of the triplet anion (derived from the antibonding $2\pi_x$ orbital of CO, Fig. 2d) is depleted via photodetachment and becomes the LUMO (π_x^*, Fig. 2b) of the neutral. Similarly, the HOMO-1 of the anion (derived from the antibonding $2\pi_y$ orbital of CO, Fig. 2c) becomes the HOMO of the neutral (π_y^*, Fig. 2a) after detachment. Thus, the extra electron of $Cu(CO)_2^-$ occupies the LUMO of $Cu(CO)_2$ while the linear conformation and orbital order are kept. A Renner–Teller distortion of linear, neutral $Cu(CO)_2$ is not evident from the calculations even though the final state cluster has a doublet electron configuration in its ground state and a degenerate HOMO. Due to the high similarity of the anionic and neutral clusters, the calculated electron affinity (1 eV) agrees perfectly with the experimentally derived adiabatic detachment energy (0.95(4) eV) and other calculations (0.89 eV)[14].

The results for $Cu(CO)_3$ are basically similar. The experimental spectrum in Fig. 1c shows a clear Franck–Condon progression ($\nu = 0$–3) on the first peak at 1 eV. A vibrational energy of 258 ± 2 meV (2081 ± 16 cm^{-1}) is deduced from the splitting. The separation to the next peak, and thus the HOMO-LUMO gap of $Cu(CO)_3$, is almost 2 eV and definetely larger than in the free Cu atom. The HOMO of the neutral and anion is a pure CO-derived orbital which is made up by one of the degenerate $2\pi^*$ orbitals of CO. A trigonal planar structure has been calculated to be the stablest isomer (D_{3h}) like in ref.[14]. The HOMO of the neutral cluster (Fig. 3b) is bonding with respect to all C atoms while it is antibonding with respect to the C–O bond, similar to the case of $Cu(CO)_2$. This agrees with a charge back-donation into the π^* orbital of CO and a reduced vibrational C–O stretching vibration with respect to triple-bonded free CO. Any Cu orbital does not contribute to the electron density of the HOMO and therefore the first peak shows

a well resolved vibrational progression of the C–O bond. The calculated vibrational energy of the totally symmetric CO mode (Raman-active) of the neutral cluster is 255 meV and agrees well with the measured value of 258 meV. The triplet configuration of $Cu(CO)_3^-$ does not converge in the calculations, like in ref.[14]. Therefore the calculated electron affinity corresponds to the energy difference between the electronic ground state of the singlet anionic cluster and doublet neutral cluster. The electron affinity has been calculated to be 1.22 eV (0.97 eV)[14]. This value is somewhat higher than the measured adiabatic electron detachment energy 1.02 eV. With respect to the electron affinity of other stable structures, the electron affinity of the trigonal planar structure of $Cu(CO)_3$, however, is the best fitting value. Upon photodetachment, the doubly occupied HOMO (π*) of the singlet anionic cluster (Fig. 3d) transforms into the singly occupied HOMO (π*) of the neutral cluster (doublet, Fig. 3b). We note that the HOMO-1 in both clusters (Fig. 3b, 3c) is bonding with respect to the Cu–C carbonyl bond and is made up by a dσ-pσ hybrid orbital in the neutral cluster and a dπ-pπ hybrid orbital in the anionic cluster (Fig. 3a, 3c). The binding energy

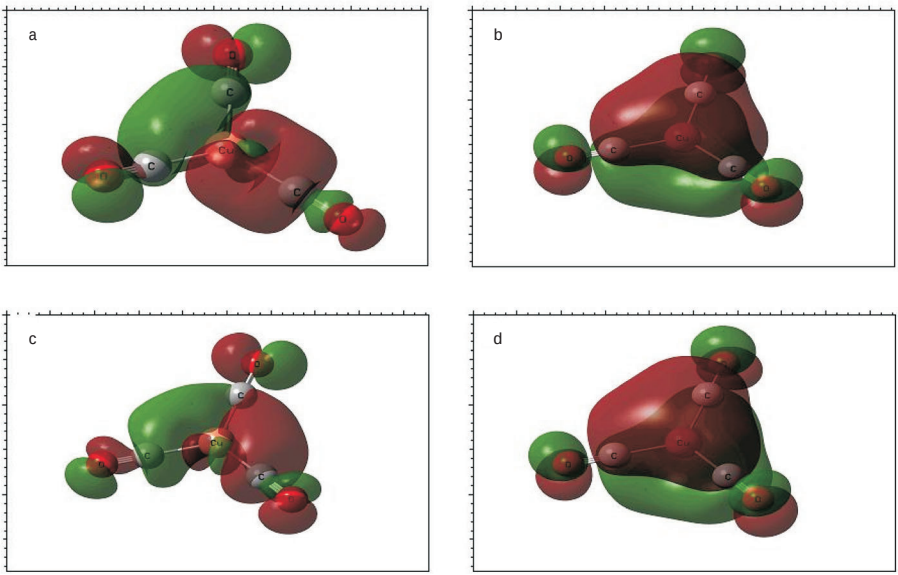

FIG. 3
Orbital contour plot of $Cu(CO)_3$ (upper panel) and $Cu(CO)_3^-$ (lower panel). HOMO-1 (a), HOMO (b), HOMO-1 (c), HOMO (d). The neutral cluster has a doublet electron configuration while the anion has a singlet ground state

of the HOMO-1 seems to be located at ≥3 eV and, therefore, only the rising edge of the peak is seen in Fig. 1c.

The results for the tetracarbonyl-copper cluster (Fig. 1d) are similar to those of the tri- and dicarbonyl-copper clusters. A well resolved vibrational splitting (ν = 0–2) is seen on the first photodetachment peak. A vibrational energy of 252 ± 8 meV (2033 ± 65 cm^{-1}) is deduced from the energy difference between ν = 0 and ν = 1. The vibrational energy is almost equal to that of $Cu(CO)_2$. In the spectrum of $Cu(CO)_4^-$, a second photodetachment is clearly visible at 2.5 eV. A vibrational splitting of ~260 ± 10 meV (2097 ± 81 cm^{-1}) is anticipated from this second peak. The experimental vibrational energy on the first photodetachment peak (252 meV) fits very well with the calculated totally symmetric C–O stretching mode of 253 meV. The vibrational splitting on the second peak seems also to be derived from the totally symmetric CO mode. The calculated HOMO and HOMO-1 of the anion are shown in Fig. 4. Like in the di- and tricarbonyl clusters, the HOMO of the anionic and neutral tetracarbonyl clusters, respectively, is a CO-derived π* orbital, antibonding with respect to the C–O bond. Cu does not visibly con-

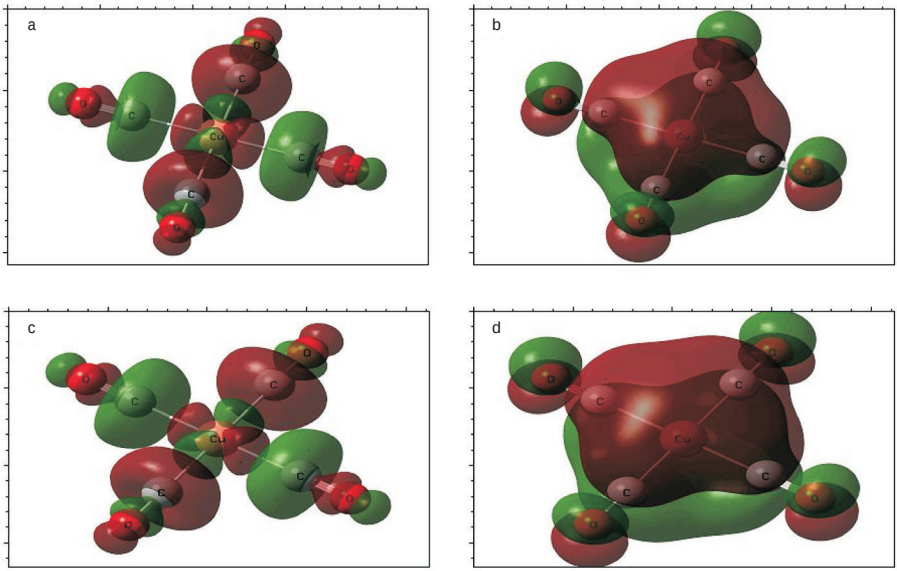

FIG. 4

Orbital contour plot of $Cu(CO)_4$ (upper panel) and $Cu(CO)_4^-$ (lower panel). HOMO-1 (a), HOMO (b), HOMO-1 (c), HOMO (d). The neutral cluster has a doublet electron configuration while the anion has a singlet ground state

tribute to the HOMO and therefore the C–O stretching vibration is clearly visible on the first peak. The HOMO-1, the origin of the second photodetachment peak, is a σ-like orbital in both the anionic and neutral cluster, which is mainly derived from the 5σ orbital of CO and partly from a 3d orbital of Cu. However, as the HOMO-1 is non bonding with respect to the Cu–C bond but bonding with respect to the C–O bond the C–O stretching vibration dominates the vibrational fine structure on the second peak at ~2.6 eV. The singlet anion is 0.8 eV more stable than the triplet anion. Upon electron detachment the doubly occupied HOMO of the anion therefore transforms into the singly occupied HOMO of the neutral cluster (doublet electron configuration). Similarly, the HOMO-1 of the anionic cluster corresponds to the HOMO-1 of the neutral cluster when switching from the singlet anion to the neutral. Thus the orbital order is equal for the neutral and anionic clusters, demonstrating that upon adding an electron to the neutral cluster, its geometry is not changed. An electron affinity of 1.4 eV has been calculated, which is ~0.4 eV higher than the experimental value (1.04(6) eV). The calculated electron affinity of the singlet configuration, however, fits better the experimental value than the electron affinity of the triplet configuration of $Cu(CO)_4^-$.

The photodetachment spectra of the dinuclear copper-carbonyl clusters are shown in Fig. 5. The peaks corresponding to the electronic transitions into the electronic ground state and the first excited state of the neutral both exhibit a vibrational fine structure. In both cases the vibrational progressions can be attributed to the C–O stretching vibration. In the case of $Cu_2(CO)_4^-$, the energy difference between the ground and first excited state of the neutral cluster is low. As a consequence, the vibrational progressions on both features overlap (Fig. 5a). Nevertheless, a vibrational splitting of 260 ± 8 meV (2097 ± 81 cm^{-1}) is deduced for the second peak and 250 ± 20 meV (2017 ± 161 cm^{-1}) is anticipated for the first peak. Thus the frequency of $Cu_2(CO)_4$ is very similar to that of $Cu(CO)_4$ making for both tetracarbonyl clusters an equal charge transfer per carbonyl ligand likely. Note that the global minimum in our calculations has D_{2h} symmetry having four equivalent ligand molecules while Li et al.[15]] calculated the low-symmetric C_s geometry to be the most stable isomer. In D_{2h} symmetry, the tetracarbonyl-dicopper cluster is composed by two CO–Cu–CO units which are bound via an intermetallic Cu–Cu bond. The measued CO frequencies fit best the calculated totally symmetric C–O stretching mode of 253 meV. All other calculated modes (IR and Raman) are deeper in energy (240–245 meV). As can be seen from the electron density plots for the tetra-

carbonyl-dicopper cluster (Fig. 6), the HOMOs of $Cu_2(CO)_4^-$ and $Cu_2(CO)_4$ are dominated by one of the CO-derived antibonding $2\pi^*$ orbitals. The anionic dicopper-carbonyls nominally have a doublet configuration in their ground state while the neutral cluster is a closed-shell species (singlet). Thus, the HOMO of the anion resembles the LUMO of the neutral cluster after electron detachment and the HOMO-1 of the anion corresponds to the HOMO of the neutral cluster after detachment as nicely seen from the

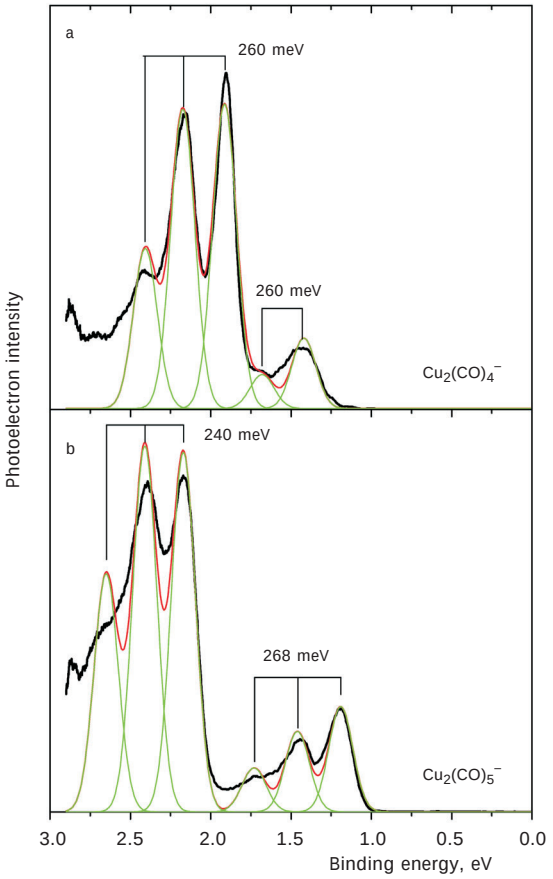

FIG. 5

Photoelectron spectra of the dicopper-carbonyl clusters $Cu_2(CO)_4^-$ (a) and $Cu_2(CO)_5^-$ (b) at a photon energy of 3.12 eV. The vibrational energy splitting is indicated by vertical black lines and the vibrational fine structure is fitted by a sum (red line) of individual Gaussian functions (green line). The experimental spectrum is shown in black

orbital contour plots in Fig. 6a–6d. The HOMO-1 of the anion is also dominated by the 2π* orbital of CO. Contributions from d-derived orbitals are marginal. Any influence on the vibrational fine structure by the Cu–C bond is not obvious in the spectra. The calculated energy difference between the neutral and anionic ground states, i.e., electron affinity, is 1.73 eV. This value, as usual in our calculations, is somewhat higher than the experimentally derived adiabatic detachment energy 1.43(9) eV.

The photodetachment spectrum of pentacarbonyl-dicopper (Fig. 5b) shows two separated photoelectron peaks at the 1.25 and 2.25 eV binding energies. On each of the peaks a vibrational splitting has been resolved. A vibrational energy of 268 ± 8 meV (2162 ± 65 cm^{-1}) and 240 ± 8 meV (1936 ± 65 cm^{-1}) has been deduced from the vibrational progression on the first and second peak, respectively. The vibrational energies agree well with the two highest calculated vibrational frequencies of the neutral cluster in its ground state. These two Raman-active modes are calculated to have an energy of 268 meV (totally symmetric) and 233 meV (CO ligands on two different subunits – see below – vibrate antisymmetrically with respect to

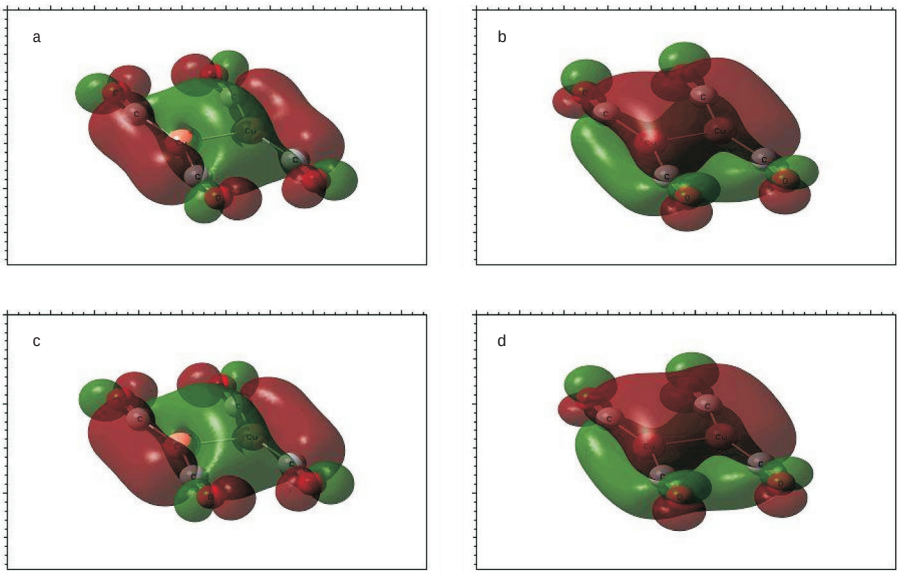

FIG. 6
Orbital contour plot of $Cu_2(CO)_4$ (upper panel) and $Cu_2(CO)_4^-$ (lower panel). HOMO (a), LUMO (b), HOMO-1 (c), HOMO (d). The neutral cluster has a singlet electron configuration while the anion has a doublet ground state

each other), respectively. The geometry has been calculated to be most stable in a relatively unsymmetrical staggered configuration[15]. Under an angle of 90°, a $Cu(CO)_2$ unit and a $Cu(CO)_3$ unit are loosely bound to each other via an intermetallic Cu–Cu bond. The HOMO orbitals of the neutral cluster and anion are depicted in Fig. 7. As in all other cases, the HOMO of the neutral and anion is derived from the 2π* orbital of CO, nonbonding with respect to the Cu–C carbonyl bond. Also, the HOMO-1 orbitals are derived from the 2π* orbital of CO. It is bonding with respect to the separated car-

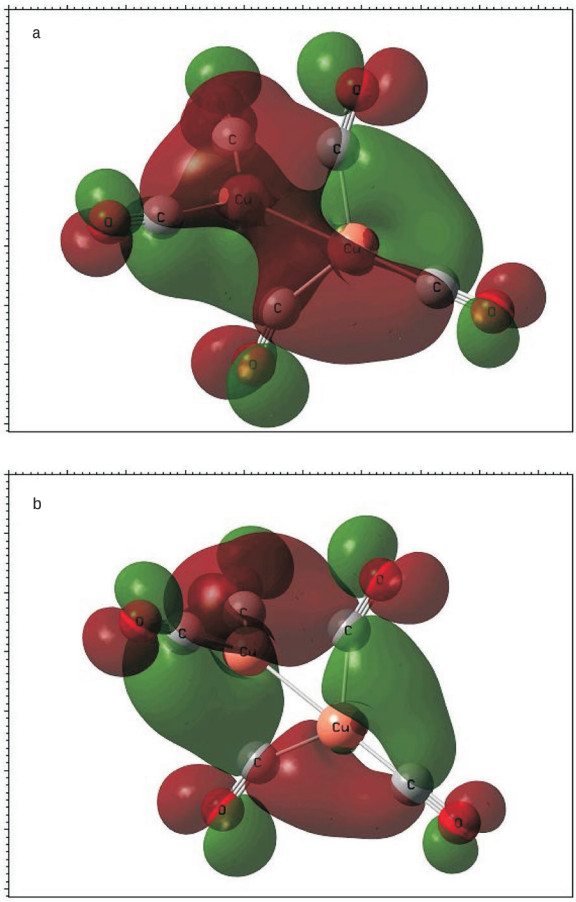

FIG. 7
Orbital contour plot of $Cu_2(CO)_5$ (upper panel) and $Cu_2(CO)_5^-$ (lower panel). HOMO (a), HOMO (b). The neutral cluster has a singlet electron configuration while the anion has a doublet ground state

bon atoms and antibonding with respect to the C–O bond. The Cu 3d orbitals participate hardly ever to the HOMO and HOMO-1. The calculated electron affinity between the doublet configuration of the anion and the singlet configuration of the neutral cluster is 1.85 eV. This value is by ~0.6 eV higher than the measured electron affinity.

CONCLUSION

For all Cu-carbonyl clusters (anionic and neutral), the HOMO corresponds to a CO-derived $2\pi^*$ orbital. Due to population of the antibonding $2\pi^*$ orbital, the experimentally resolved C–O vibrational frequency is smaller than that of free CO, in which the $2\pi^*$ orbital is totally vacant. As shown by the orbital density plots, the HOMO is nonbonding with respect to the metal–CO carbonyl bond and bonding with respect to the C atoms of the surrounding carbonyls. As the $2\pi^*$ orbital is filled by back-donation from the metal, the Cu orbitals are pushed down in binding energy (>3 eV) with respect to the orbital binding energy of a free Cu atom. In contrast to anionic Pt_n-carbonyl and Au_n-carbonyl clusters[18,19], vibrational fine structure (C–O stretching vibration) has been observed for all copper-carbonyl clusters. This comes along with a completed d-shell in the Cu-carbonyl clusters. In Pt-carbonyl clusters, the vibrational splitting of the C–O bond is seen only in case of saturation, i.e. if the intrametallic charge redistribution from s→d leads to a complete d-shell[18]. In agreement with ref.[15], (Cu–CO–Cu)-bridging bonds are not favoured in our calculations for the dinuclear copper-carbonyl clusters. Except for $Cu(CO)_2$, the measured vibrational energy on the first photodetachment peak agrees best with the totally symmetric C–O vibrational mode of the neutral cluster. For $Cu_2(CO)_5$ a second Raman mode has been resolved. Except for $Cu(CO)_3$, no Cu–CO bonding orbital has been observed within the two lowest-lying frontier orbitals (HOMO, HOMO-1). $d\pi$-$p\pi$ M–CO carbonyl bonds have been calculated to appear at a binding energy > 5 eV. The copper 4s orbital is destabilized in the carbonyls and is pushed up into the virtual orbital space as turns out by our calculations. Therefore the electrons from the 4s shell must be back-donated to the carbonyls. The dicopper-carbonyls are bonded via a Cu–Cu d-derived intermetallic bond rather than via a $4s\sigma$ bond. The electron affinity slightly increases with the number of CO ligands for the monocopper-carbonyl clusters. Also, the electron affinity is usually overestimated by our calculations with respect to the experimental value, which might be due to relativistic reasons.

REFERENCES

1. Bonacic-Koutecky V., Fantucci P., Koutecky J.: *J. Chem. Phys.* **1989**, *91*, 3794.
2. Bonacic-Koutecky V., Fantucci P., Koutecky J.: *J. Chem. Phys.* **1990**, *93*, 3802.
3. Bonacic-Koutecky V., Fantucci P., Koutecky J.: *Z. Phys. Chem. N. F.* **1990**, *169*, 35.
4. Bonacic-Koutecky V., Fantucci P., Koutecky J.: *Chem. Rev.* **1991**, *91*, 1035.
5. Bonacic-Koutecky V., Cespiva L., Fantucci P., Pittner J., Koutecky J.: *J. Chem. Phys.* **1994**, *100*, 490.
6. Brown D. M., Bhatt B. L., Hsiung T. H., Lewnard J. J., Waller F. J.: *Catal. Today* **1991**, *8*, 279.
7. Blyholder G.: *J. Phys. Chem.* **1964**, *68*, 2772.
8. Bauschlicher C. W., Bagus P. S.: *J. Chem. Phys.* **1984**, *81*, 5889.
9. Nitschke F., Ertl G., Küppers J.: *J. Chem. Phys.* **1981**, *74*, 5911.
10. Lüttgens G., Pontius N., Friedrich C., Klingeler R., Bechthold P. S., Neeb M., Eberhardt W.: *J. Chem. Phys.* **2001**, *114*, 8414.
11. Pontius N., Bechthold P. S., Neeb M., Eberhardt W.: *Appl. Phys. B: Lasers Opt.* **2000**, *71*, 351.
12. Moore C.: *Atomic Energy Levels*, Vol. III (*Molybdenum through Lanthanum and Hafnium through Actinium*), Circular of the National Bureau of Standards 467. U. S. Government Printing Office, Washington, D. C. 1958.
13. Frisch M. J., Trucks G. W., Schlegel H. B., Scuseria G. E., Robb M. A., Cheeseman J. R., Zakrzewski V. G., Montgomery J. A., Stratmann R. E., Burant J. C., Dapprich S., Millam J. M., Daniels A. D., Kudin K. N., Strain M. C., Farkas O., Tomasi J., Barone V., Cossi M., Cammi R., Mennucci B., Pomelli C., Adamo C., Clifford S., Ochterski J., Petersson G. A., Ayala P. Y., Cui Q., Morokuma K., Salvador P., Dannenberg J. J., Malick D. K., Rabuck A. D., Raghavachari K., Foresman J. B., Cioslowski J., Ortiz J. V., Baboul A. G., Stefanov B. B., Liu G., Liashenko A., Piskorz P., Komaromi I., Gomperts R., Martin R. L., Fox D. J., Keith T., Al-Laham M. A., Peng C. Y., Nanayakkara A., Challacombe M., Gill P. M. W., Johnson B., Chen W., Wong M. W., Andres J. L., Gonzalez C., Head-Gordon M., Replogle E. S., Pople J. A.: *Gaussian 03*. Pittsburgh (PA) 2003.
14. Wu G., Li Y. W., Xiang H. W., Xu Y. Y., Sun Y. H., Jiao H.: *J. Mol. Struct. (THEOCHEM)* **2003**, *637*, 101.
15. Li Q., Liu Y., Xie Y., King B., Schaefer H. F.: *Inorg. Chem.* **2001**, *40*, 5842.
16. Ganteför G., Cha C. Y., Handschuh H., Schulze Icking-Konert G., Kessler B., Gunnarsson O., Eberhardt W.: *J. Electron Spectrosc. Relat. Phenom.* **1995**, *76*, 37.
17. Huber K. P., Herzberg G.: *Molecular Spectra and Molecular Structure*, Vol IV. Van Nostrand Reinhold, New York 1979.
18. Schulze Icking-Konert G., Handschuh H., Ganteför G., Eberhardt W.: *Phys. Rev. Lett.* **1996**, *76*, 1047.
19. Zhai H. J., Kiran B., Dai B., Li J., Wang L. S.: *J. Am. Chem. Soc.* **2005**, *127*, 12098.